

# Mechanics Based Design of Structures and Machines

## An International Journal

ISSN: 1539-7734 (Print) 1539-7742 (Online) Journal homepage: <http://www.tandfonline.com/loi/lmbd20>

## Dimensionless design model for biaxial Cartwheel flexure hinges

Zongxuan Li, Xue Chen & Guang Jin

To cite this article: Zongxuan Li, Xue Chen & Guang Jin (2018) Dimensionless design model for biaxial Cartwheel flexure hinges, *Mechanics Based Design of Structures and Machines*, 46:4, 401-409, DOI: [10.1080/15397734.2017.1341841](https://doi.org/10.1080/15397734.2017.1341841)

To link to this article: <https://doi.org/10.1080/15397734.2017.1341841>



Accepted author version posted online: 21 Jun 2017.  
Published online: 17 Jul 2017.



Submit your article to this journal [↗](#)



Article views: 72



View related articles [↗](#)



View Crossmark data [↗](#)



# Dimensionless design model for biaxial Cartwheel flexure hinges

Zongxuan Li , Xue Chen, and Guang Jin

Changchun Institute of Optics, Fine Mechanics and Physics, Chinese Academy of Sciences, Changchun, China

## ABSTRACT

Flexure hinges have been widely used in space-borne telescopes for mounting reflective optics with high surface figure requirements. To realize the three-point flexural mount of a  $\Phi 750$  mm primary mirror, a Cartwheel biaxial flexural hinge composed by filleted short beams is proposed and the dimensionless design graph method for the flexural hinge is presented. The finite element analysis is performed on the flexure model to validate the proposed method. We also demonstrate the feasibility of the proposed method experimentally. The maximum relative error of the rotational stiffness between analysis, testing result, and design value is 5.0%. The proposed dimensionless design graph can be used as a design tool to determine the optimal geometry of a spatial flexure hinge rapidly.

## ARTICLE HISTORY

Received 24 February 2017  
Accepted 9 June 2017

## KEYWORDS

Dimensionless design; finite element method; flexure hinge; mirror mount; rotational stiffness



## 1. Introduction

Traditional hinge allows rotational degree of freedom between connected parts in mechanism. However, the inherent clearance between mating parts causes backlash. In addition, the relative motion in hinge joints causes friction, leading to wear, creep, and increased clearances. A kinematical chain of such joints with motion errors will result in poor accuracy and repeatability (Howell, 2001; Lobontiu, 2003).

A flexure hinge is manufactured from one piece of monolithic material and acts as the weak segment between two relatively rigid parts. It can utilize the inherent compliance of a material rather than restrain the deformation. Despite the infinite rotational range, flexure hinge eliminates the presence of friction, backlash, and wear, it also avoids maintenance, lubrication, and assembly. Further benefits include submicron accuracy due to the flexure's continuous monolithic construction. The accuracy is important in many micro, nano, and biomedical applications, such as microelectromechanical systems (MEMS), optical engineering, robotics, biomedical engineering, and aerospace engineering (Yina et al., 2004; Ansola et al., 2010; Rijnveld and Pijnenburg, 2010; Kim et al., 2012; Lobontiu, 2014; Munteanu et al., 2016).

Flexure hinges can be divided into three types according to the numbers of the rotational axis: single-axis hinge, two-axis hinge, and multi-axis hinge. The fundamental single-axis hinge can be further categorized into several subgroups: leaf flexure hinge, circular flexure hinge, parabolic flexure hinge, hyperbolic flexure hinge, and elliptical flexure hinge according to the cross-sectional contour of flexures. Complex flexure is typically composed of multiple basic flexures above, for example, cross-strip flexure, split-tube flexure, and cartwheel flexure.

Cartwheel flexure hinge, also known as Haberland flexure hinge Lemke et al. (1999), belongs to the single-axis complex flexure. The cruciform flexure consists of four identical blade-type flexures. The intersection point is considered as the pivot of the flexure. It has the merits such as large rotational range, low center shift of pivot, low stress concentration, high antibuckling stiffness, and ease of manufacturing. A biaxial Cartwheel flexural hinge can be obtained by cutting a monolithic hollow metal cylinder along

**CONTACT** Zongxuan Li  [lizongx@hotmail.com](mailto:lizongx@hotmail.com)  Changchun Institute of Optics, Fine Mechanics and Physics, Chinese Academy of Sciences, Changchun 130033, China.

Color versions of one or more of the figures in this article can be found online at [www.tandfonline.com/lmbd](http://www.tandfonline.com/lmbd).

Communicated by Javier Cuadrado.

© 2017 Taylor & Francis

two orthogonal directions, respectively, using electrodischarge machining (EDM) method. Two identical flexures are machined simultaneously in the first machining step. Then the cylinder is rotated 90 degrees with respect to the axis and machined for the other two flexures. This design can reduce the complexity of assembling and the separation slot will limit the rotational angle, protecting the flexure from yielding.

There are several papers discussing the design equations of Cartwheel flexure hinge. Smith (2000) derived the closed-form stiffness equation based on Euler–Bernoulli beam theory. Schotborgh et al. (2005) derived the in-plane stiffness equations using dimensionless design method. Bi et al. (2009) developed the accurate model including the load cases of a bending moment combining with a horizontal and a vertical force by the superposition of two triangular flexure pivot. Pei et al. (2009) derived the rotational stiffness equations based on pseudo-rigid-body model. Wu et al. (2015) derived a 6-DOF compliance model of the generalized cartwheel flexure hinge. Markovic and Zelenika (2016) investigated the parasitic shifts and stiffness variations of cross-spring through nonlinear finite element analysis (FEA) methods, those research focused on the in-plane Cartwheel flexure with thin beams. It would be difficult to derive the close-form equations for the biaxial Cartwheel flexure, which is a 3-dimensional flexure.

In this paper, we propose a biaxial Cartwheel flexure hinge with filleted short beams for the three-point flexural mount of a  $\Phi 750$  mm SiC primary mirror of a space-borne telescope. The flexure can efficiently release the thermal stress caused by coefficient of thermal expansion (CTE) inconsistency of structures and maintain the static and dynamic rigidity of the mirror assembly. Then we present a dimensionless design method for the biaxial hinge to investigate the relationship between geometry parameters and stiffness graphically and numerically. Finally, this design method is validated by both finite element method and experiment. This design method can enable the designer to quickly choose the flexure type and determine the geometry parameters during the initial design process.

## 2. Cartwheel biaxial flexural hinge

The  $\Phi 750$  mm primary mirror is the crucial reflective optics of a Kosch type, three-mirror anastigmatic space-borne telescope. This mirror is fabricated from reaction-bonded silicon carbide material by gel-casting method and the lightweight ratio reaches 80%. The acceptance requirements on the mirror surface error is 9 nm RMS ( $\lambda/60$ ). Three equally arranged flexures mount the mirror to the baseplate, which is the mechanical interface to optical bench of the telescope shown in Figure 1a. The flexure mount functions in three aspects: (a) compensating the thermal expansion difference between mirror and telescope structure without distorting mirror surface; (b) keeping precisely the surface figure of mirror from on-ground optical testing to on-orbit operation; and (c) releasing the mechanical stress induced by alignment adjusting and imperfection of fabrication. Furthermore, the mounting flexures should make survive the dynamic loads including random vibration and shock and maintain the surface figure during fabrication by computer controlled optical surfacing (CCOS) as shown in Figure 1b.

The optimal geometry design process of the flexure comprises a series of complex iterations of multiobjective structural optimization (Kihm and Yang, 2013; Wu et al., 2015). The mirror surface error under load cases of gravity combined with thermal variation and the natural frequency of the assembly (usually higher than 100 Hz) are the main optimization objectives (Kihm et al., 2012). The sensitivity analysis performed on the mirror will provide initial design requirements to the stiffness of flexure. As the starting point of optimization process, an appropriate initial structural design is important, so that the design cycles could be effectively shortened.

The proposed biaxial Cartwheel flexural hinge for mirror mounting is shown in Figure 2. The structural parameters which determine the mechanical characteristics are illustrated in Figure 2a, where  $L$  denotes beam length,  $R$  is the radius of curvature of fillet,  $h$  is the height of beam, and  $t$  is the thickness of hollow cylinder which is not shown in the figure. Utilizing the electrodischarging machining method, the flexural hinge is obtained from one monolithic hollow cylinder. Four filleted short beams converging to one virtual point compose the Cartwheel flexure and four Cartwheel flexures equally arranged with respect to the  $z$  axis, functioning together as a biaxial hinge. Under a moment load  $M$ , the Cartwheel

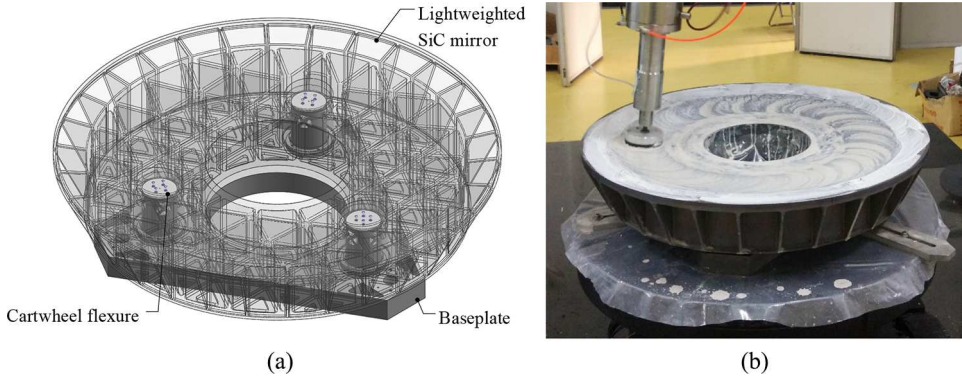


**Figure 1.** Schematic view of lightweight mirror mounted by Cartwheel flexural hinges. (a) The flexural mount configuration of a space mirror, (b) mirror assembly being optical polished.

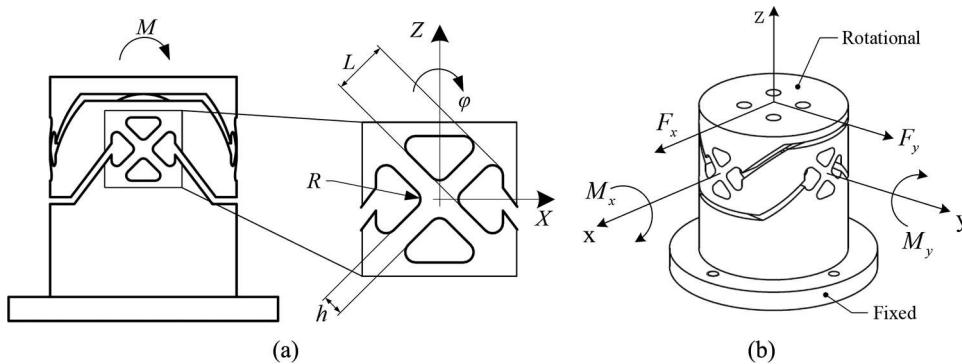


**Figure 2.** The biaxial Cartwheel flexure hinge and its design parameters. (a) Biaxial Cartwheel flexural hinge with filleted beams, (b) Coordinate system of biaxial Cartwheel flexure hinge.

flexure will deflect and the upper part will rotate an angle  $\varphi$  with respect to the lower fixed part. Four slits separate the rotational part from the fixed part to provide two rotational degrees of freedom. Meanwhile the slits can also act as the geometric limit of the hinge's deflection to prevent yielding. Four Cartwheel flexures are machined based on the same nominal dimensions to provide the identical biaxial mechanical behaviors. The Cartesian coordinate system is shown in Figure 2b. The designed flexure provides compliance mainly in two directions:  $x$  and  $y$  axes. Lateral forces  $F_x$  and  $F_y$ , as well as moments  $M_x$  and  $M_y$ , are the loads mainly considered in this paper.

### 3. Dimensionless design equations

To investigate the relationship between flexure geometry and its mechanical behavior, dimensionless design method is utilized to assist designer in the process of choosing flexure type and determining the initial structural parameters in the starting phase of optimization (Tian et al., 2010; Ditolla et al., 1986; Tufekci et al., 2016). Table 1 shows the variable parameters included in the dimensionless modeling procedure.

**Table 1.** Nomenclature.

$C$	$E$	$R$	$L$	$h$	$t$	$k$	$\varphi$	$\sigma$	$x, y, z$
Translational stiffness	Young's modulus	Fillet radius	Beam length	Beam height	Cylinder thickness	Rotational stiffness	Rotational angle	Maximum stress (rotational)	Coordinate axes

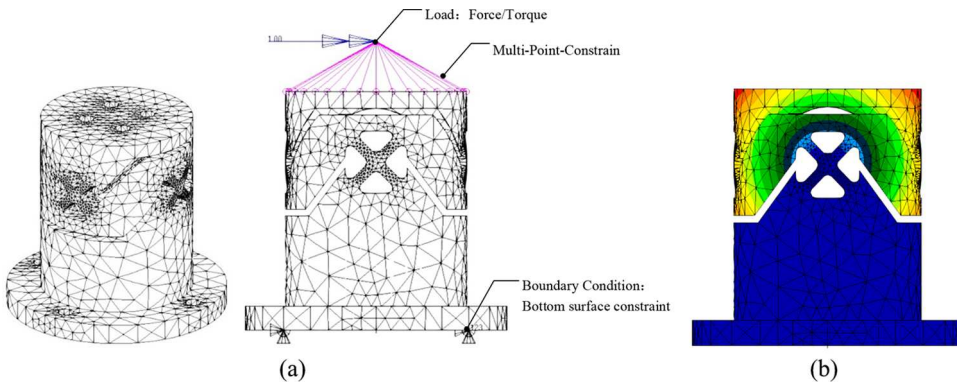


**Figure 3.** Finite element analysis for dimensionless design graph. (a) Finite element model of flexure including loads/BCs, (b) Displacement fringe of an analysis result.

The dimensionless design graph is calculated by polynomial fitting to the parametric finite element analysis results of the flexure. FEA computer program NASTRAN is utilized to solve the parametric model. The important aspects about the analysis using NASTRAN are summarized as follows:

- (a) Program version: MD NASTRAN 2010.1.
- (b) Element type: TET10 (CTETRA in NASTRAN).
- (c) Material property: The flexure is manufactured from an Invar steel block, marked by Chinese Standards “3J53”. The Young’s modulus of the material is  $206 \times 10^9$  Pa, and Poisson ratio is 0.28.

Based upon numerous analysis results on a single-filletted short beam flexure, when  $R = 0.7h$ , the beam flexure element possesses maximal angle–stress ratio (Schotborgh et al., 2005). This means that the maximum rotation angle can be realized with a cost of minimum stress. Therefore  $R = 0.7h$  is used as the optimal radius of fillet. There remain only three independent parameters to determine a specific Cartwheel biaxial flexure: the thickness of hollow cylinder ( $t$ ), height of a single beam in Cartwheel flexure ( $h$ ), and its length ( $L$ ). The parametric analysis is performed on the FEM model of flexure based on the various combinations of  $t$ ,  $h$ , and  $L$ .

The finite element model of the biaxial hinge is built using the preprocessor software MSC/PATRAN. The grid density at the flexure corners has been increased to enhance computational accuracy, as shown in Figure 3a. A torque load with a unit force/moment is applied to the rotational part of the flexure. The fixed part is constrained by restricting the nodes on the bottom surface. A single node which is 10 mm offset above the top surface of the flexure is created as the independent term. All the nodes on the top surface are dependent terms and all the three translational DoFs of every node are associated to build a RBE2 type multipoint constrain (MPC). Then a unit load is applied to the independent node to deflect the flexure. The analysis result under a unit moment load is depicted in fringe form shown in Figure 3b.

Then, the dimensionless number  $\varepsilon$  is defined as the square root of the ratio of beam height ( $h$ ) and length ( $L$ ):

$$\varepsilon = \sqrt{h/L}. \quad (1)$$

The square root of the ratio  $h/L$  is the dimensionless number only for enlarging the clarity of curve display when the ratio is relatively small. To investigate the relationship between geometric dimensions and mechanical behavior of Cartwheel flexure hinge, we perform polynomial fitting to large amounts of FEM analysis data by least square method. For each curve fitting, 20 data points have been calculated, and the incremental step of  $\varepsilon$  is set to 0.02. The advantage of this method is that we do not have to choose a continuous series of numbers for the value combinations of  $t$ ,  $h$ , and  $L$  for polynomial fitting, we just need to make sure the  $\varepsilon$  value ( $\sqrt{h/L}$ ) is what we want. Therefore, it is not necessary to specify the range of variation of each geometric parameter. Because, in the dimensionless design equations, all

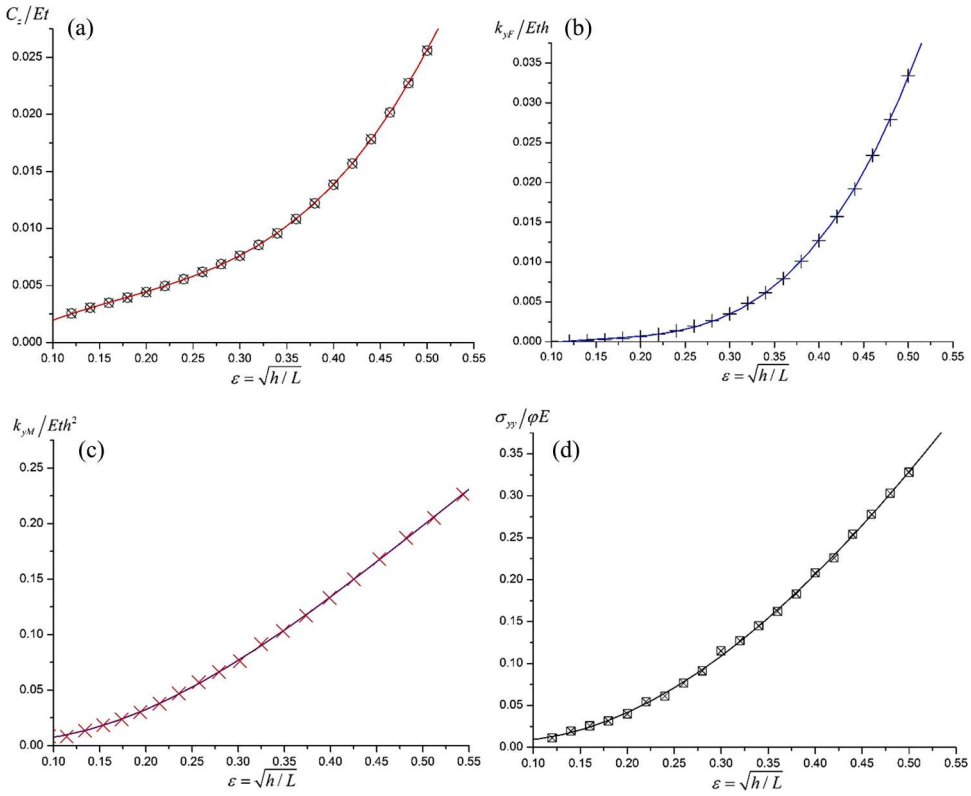


**Figure 4.** Dimensionless design graph for Cartwheel biaxial flexural hinge. (a) Dimensionless stiffness in axial direction, (b) dimensionless rotational stiffness under lateral force  $F$ , (c) dimensionless rotational stiffness under moment  $M$ , (d) dimensionless rotational stress caused by rotation.

dimensions are cancelled and absolute quantities are meaningless. These equations unveil the relative numerical relationships between the physical quantities. This is the unique advantage of the technique. Here we choose the third-order polynomials rather than higher ones, because higher order polynomials will not improve the residual error of the curve fitting prominently (Bi et al., 2010). Figure 4 shows the dimensionless design graph of biaxial Cartwheel flexure hinge according to the third-order polynomial fitting equations. The original data points from FEA results are shown as spots in each figure, respectively.

The dimensionless design equations for the flexural hinge corresponding to Figure 4 are listed as follows:

Dimensionless stiffness in  $z$  direction  $C_z$ :

$$\frac{C_z}{Et} = \frac{F}{zEt} = -0.0023 + 0.0597\varepsilon - 0.21\varepsilon^2 + 0.4048\varepsilon^3. \quad (2)$$

Dimensionless rotational stiffness under the force  $F$  in  $x$  direction  $k_{xF}$ :

$$\frac{k_{xF}}{Eth} = \frac{F}{\varphi Eth} = -0.0037 + 0.0645\varepsilon - 0.3665\varepsilon^2 + 0.77\varepsilon^3. \quad (3)$$

Dimensionless rotational stiffness under the moment  $M$  in  $y$  direction  $k_{yM}$ :

$$\frac{k_{yM}}{Eth^2} = \frac{M}{\varphi Eth^2} = 0.0081 - 0.1930\varepsilon + 1.5108\varepsilon^2 - 1.0291\varepsilon^3. \quad (4)$$

Dimensionless rotational stress  $\sigma_{yy}$ :

$$\frac{\sigma_{yy}}{\varphi E} = 0.0176 - 0.3019\varepsilon + 2.2783\varepsilon^2 - 0.8608\varepsilon^3. \quad (5)$$

#### 4. Case study

A design case is presented to illustrate how to use the dimensionless graph or equations to perform a quick design process for an initial structure layout. Considering a biaxial Cartwheel flexure hinge which rotates from  $-0.66^\circ$  to  $+0.66^\circ$  (total angle  $1.32^\circ$ ), through sensitivity analysis on the mirror assembly under the load of unit moment/shear force, we conclude that the translational stiffness along  $z$  axis and rotational stiffness should meet:

$$C_z > 7.0 \times 10^7 \text{ N/m} \quad (6)$$

$$k_{yM} \leq 3000 \text{ Nm/rad} \quad (7)$$

According to the handbook of metal material (Liu, 2017), the allowable stress of Invar steel is 1,200 MPa. The dimensionless number corresponding to the stress limit can be calculated:

$$\frac{\sigma_{yy}}{\varphi E} = 0.5026. \quad (8)$$

Combining Eq. (8) with Eq. (5), we can solve the cubic equation of  $\varepsilon$

$$\varepsilon = \sqrt{h/L} = 0.6211. \quad (9)$$

Substituting Eq. (9) into Eq. (2), we obtain

$$\frac{C_z}{t} = 1.045 \times 10^{10} \text{ Pa}. \quad (10)$$

According to Eq. (6), we can get the lower limit of  $t$

$$t > 6.70 \text{ mm}. \quad (11)$$

It is obvious that a smaller value of  $t$  will result in a lower mass of the flexure hinge, which could be more attractive in engineering application. Substituting  $t = 7 \text{ mm}$  into Eq. (10) leads to

$$C_z = 7.320 \times 10^7 \text{ N/m}. \quad (12)$$

With the height  $h$  as the remaining uncertain parameters, we substitute Eqs. (9) and (11) into Eq. (4) and obtain

$$\frac{k_{yM}}{h^2} = 3.237 \times 10^8 \text{ N/m} \quad (13)$$

Considering Eq. (7), the  $h$  value can be calculated

$$h \leq 3.04 \text{ mm}. \quad (14)$$

With  $h = 3 \text{ mm}$ , we can obtain  $L = 7.78 \text{ mm}$  and  $k_{yM} = 2912.01 \text{ Nm/rad}$  by solving Eq. (4). All the parameters of Cartwheel biaxial flexure in the design case have been determined, as shown in Table 2.

**Table 2.** Parameters of the design case.

Parameters	$\varepsilon$	$R/\text{mm}$	$L/\text{mm}$	$h/\text{mm}$	$t/\text{mm}$	$\varphi/\text{degree}$	$k_{yM}/(\text{Nm/rad})$	$C_z/(\text{N/m})$
Value	0.6211	2.1	7.78	3	7	$0.66^\circ$	2912.01	$7.32 \times 10^7$



## 5. Design validation

### 5.1. Finite element method

We use the FEA software MD/NASTRAN to validate the dimensionless design equations about the stiffness of hinge and the design process. Although the dimensionless design equations are calculated by fitting the scattered FEA results, the simulation validation still makes sense. As we stated in Section 3, the parametric values of  $t$ ,  $h$ , and  $L$  can be chosen randomly, but the  $\varepsilon$  values should have an incremental step of 0.02. The parameter values calculated in Table 2 may deviate from the fitting spots substantially. Therefore, the FEA simulation can validate the applicability of dimensionless equations effectively. The simulation process is the same as that presented in Section 4. The node displacement along  $z$  on the edge of hinge cylinder is given by NASTRAN  $\Delta Z = 9.68 \times 10^{-6}$  mm. The rotational stiffness  $k'_{yM}$  about  $y$  axis can be derived by substituting  $\Delta Z$  into Eq. (15)

$$k'_{yM} = \frac{M}{\theta} = \frac{M\Phi}{2\Delta Z} = 2893.21 \text{ Nm/rad.} \quad (15)$$

where  $M$  is the unit moment load and  $\Phi = 56$  mm is the outer diameter of the hinge cylinder.

### 5.2. Experiment and results

To validate the dimensionless design method for biaxial Cartwheel flexure hinge experimentally, a test piece of the designed flexure made of Invar Steel 3J53 is manufactured as shown in Figure 5a. The experimental layout is shown in Figure 5b.

The optical test setup is comprised of a vibration isolation optical table, a test piece of flexure hinge, a reflective mirror, a lever arm, an electronic autocollimator for angle measurement, and a series of load mass. The fixed part of the flexure hinge is bolted to the table surface by four screws. The lever arm bonded with a mirror is fastened to the top surface of the hinge. The autocollimator is fixed to the table next to the hinge. No matter where the exact location of the mirror relative to the hinge is, the rotational angles of the two objects are the same because of the measurement principle of the autocollimator. A series of steel blocks simulating load mass is hang to one end of the lever arm. The gravity of the load mass applied to the hinge will generate a moment load to the flexure (Chen et al., 2009). The electronic autocollimator TriAngle<sup>®</sup> monitors the tilting angle of the mirror with respect to the increments of load mass and displays the real-time angle results on screen. In the testing process, the load mass increases with a step of 200 g. The load ranges from 200 to 2,200 g to measure the variant angles of flexure hinge under different loads.

The test results are listed in Table 3, where  $\gamma$  denotes the absolute angle that has been measured and  $\theta$  denotes the incremental angle for each load step.

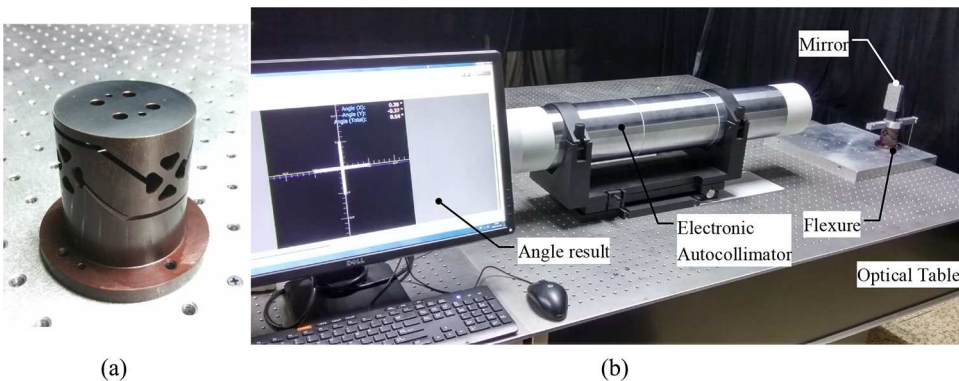


Figure 5. The optical test layout for the test piece of designed flexure. (a) Test piece of the flexure, (b) the optical test setup.



**Table 3.** Experimental results of rotational angle of flexure.

Load case	1	2	3	4	5	6	7	8	9	10	11	Ave	RMS
Load mass (g)	200	400	600	800	1,000	1,200	1,400	1,600	1,800	2,000	2,200	–	–
$\gamma$ (")	410.52	395.85	381.05	366.85	352.31	337.72	323.34	308.54	293.89	279.52	264.76	–	–
$\theta$ (")	–	14.67	14.8	14.2	14.54	14.59	14.38	14.8	14.65	14.37	14.76	14.58	0.20

**Table 4.** Comparison between results of rotation stiffness.

Rotational stiffness (Nm/rad)	Design value	Simulation value	Test value
	2912.01	2893.21	2772.84

The average value of the incremental angle 14.58" is chosen as the flexure hinge tilting angle caused by the load mass of 200 g. Then the experimental value of rotational stiffness  $k_{y\theta}$  can be calculated in Eq. (16), where the lever arm  $l = 0.11$  mm and  $F_G = 1.96$  N (the gravity force by 200 g load mass)

$$k_{y\theta} = \frac{lF_G}{\theta} = 2772.84 \text{ Nm/rad.} \quad (16)$$

Table 4 shows the comparison between design value, simulation value, and test value of Cartwheel flexure hinge. The maximum relative error is only 5.0%. These results successfully validate the engineering application of dimensionless design method for biaxial Cartwheel flexure hinge.

## 6. Conclusion

To satisfy the critical mounting requirements of a lightweight mirror in a space telescope, a Cartwheel biaxial flexure hinge is proposed in this paper as the three-point support element. Driven by the motivation of shortening the optimization cycle of the flexure's multiple parameters, we present a dimensionless design method for the biaxial flexure hinge. The design method is validated both by finite element analysis using MD/NASTRAN and experiment using an autocollimator. The results show that the maximum relative error is 5.0%, indicating the prospect of application in precision space optomechanical system design process. In the future, we will investigate the global dimensionless design model including the geometric parameters of lightweight mirror and evaluate the performance under the impact such as surface figure error and natural frequency, rather than the stiffness of a flexure.

## Funding

This research was supported by National 863 High Technology Research & Development Program of China (No. 2015AA7015090).

## ORCID

Zongxuan Li  <http://orcid.org/0000-0001-5239-6789>

## References

- Ansola, R., Vegueria, E., Maturana, A. (2010). 3D compliant mechanisms synthesis by a finite element addition procedure. *Finite Elements in Analysis and Design* 46:760–69. doi:10.1016/j.finel.2010.04.006
- Bi, S., Zhao, H., Yu, J. (2009). Modeling of a cartwheel flexural pivot. *Journal of Mechanical Design* 131:061010. doi:10.1115/1.3125204
- Bi, S., Zhao, S., Zhu, X. (2010). Dimensionless design graphs for three types of annulus-shaped flexure hinges. *Precision Engineering* 34:659–66. doi:10.1016/j.precisioneng.2010.01.002
- Chen, G., Liu, X., Gao, H. (2009). A generalized model for conic flexure hinges. *Review of Scientific Instrument* 80:055106. doi:10.1063/1.3137074

- Ditolla, R., Richard, R. M., Vukobratovich, D. (1986). Design of a support system for the primary mirror of a cryogenic space telescope. *SPIE* 619:176–81. doi:[10.1117/12.966651](https://doi.org/10.1117/12.966651)
- Howell, L.L. (2001). *Compliant Mechanisms*. New York: Wiley.
- Kihm, H., Yang, H. (2013). Design optimization of a 1-m lightweight mirror for a space telescope. *Optical Engineering* 52:091806. doi:[10.1117/1.OE.52.9.091806](https://doi.org/10.1117/1.OE.52.9.091806)
- Kihm, H., Yang, H., Moon, K. (2012). Adjustable bipod flexures for mounting mirrors in a space telescope. *Applied Optics* 51:7776–83. doi:[10.1364/AO.51.007776](https://doi.org/10.1364/AO.51.007776)
- Kim, H., Ahn, D., Gweon, D. (2012). Development of a novel 3-degrees of freedom flexure based positioning system. *Review of Scientific Instrument* 83:055114. doi:[10.1063/1.4720410](https://doi.org/10.1063/1.4720410)
- Lemke, D., Grözinger, U., Krause, O. (1999). Focal plane chopper for the PACS instrument aboard the far infrared space telescope FIRST. *SPIE* 3759:205–13. doi:[10.1117/12.372697](https://doi.org/10.1117/12.372697)
- Liu, S. (2017). *Practical Handbook of Metal Materials*. Beijing: China Machine Press.
- Lobontiu, N. (2003). *Compliant Mechanisms: Design of Flexure Hinges*. New York: CRC Press.
- Lobontiu, N. (2014). Out-of-plane (diaphragm) compliances of circular-axis notch flexible hinges with midpoint radial symmetry. *Mechanics Based Design of Structures and Machines* 42:518–38. doi:[10.1080/15397734.2014.899152](https://doi.org/10.1080/15397734.2014.899152)
- Markovic, K., Zelenika, S. (2016). Optimized cross-spring pivot configurations with minimized parasitic shifts and stiffness variations investigated via nonlinear FEA. *Mechanics Based Design of Structures and Machines* 44. doi:[10.1080/15397734.2016.1231614](https://doi.org/10.1080/15397734.2016.1231614)
- Munteanu, M. G., Bona, F. D., Bressan, F. (2016). Shaft design: A semi-analytical finite element approach. *Mechanics Based Design of Structures and Machines* 44. doi:[10.1080/15397734.2017.1322976](https://doi.org/10.1080/15397734.2017.1322976)
- Pei, X., Yu, J., Zong, G. (2009). The modeling of cartwheel flexural hinges. *Mechanism and Machine Theory* 44:1900–09. doi:[10.1016/j.mechmachtheory.2009.04.006](https://doi.org/10.1016/j.mechmachtheory.2009.04.006)
- Rijnveld, N., Pijnenburg, J. (2010). Picometer stable scan mechanism for gravitational wave detection in space. *SPIE* 7734:77341R. doi:[10.1117/12.857040](https://doi.org/10.1117/12.857040)
- Schotborgh, W. O., Kokkeler, F. G., Tragter, H. (2005). Dimensionless design graphs for flexure elements and a comparison between three flexure elements. *Precision Engineering* 29:41–47. doi:[10.1016/j.precisioneng.2004.04.003](https://doi.org/10.1016/j.precisioneng.2004.04.003)
- Smith, S. T. (2000). *Flexures: Elements of Elastic Mechanisms*. New York: Gordon and Breach Science Publishers.
- Tian, Y., Shirinzadeh, B., Zhang, D. (2010). Three flexure hinges for compliant mechanism designs based on dimensionless graph analysis. *Precision Engineering* 34:92–100. doi:[10.1016/j.precisioneng.2009.03.004](https://doi.org/10.1016/j.precisioneng.2009.03.004)
- Tufekci, E., Eroglu, U., Aya, S. A. (2016). Exact solution for in-plane static problems of circular beams made of functionally graded materials. *Mechanics Based Design of Structures and Machines* 44(4):476–94. doi:[10.1080/15397734.2015.1121398](https://doi.org/10.1080/15397734.2015.1121398)
- Wu, J., Cai, S., Cui, J. (2015). A generalized analytical compliance model for cartwheel flexure hinges. *Review of Scientific Instrument* 86:105003. doi:[10.1063/1.4934199](https://doi.org/10.1063/1.4934199)
- Yina, L., Ananthasuresha, G. K., Ederb, J. (2004). Optimal design of a cam-flexure clamp. *Finite Elements in Analysis and Design* 40:1157–73. doi:[10.1016/j.finel.2003.08.005](https://doi.org/10.1016/j.finel.2003.08.005)